A Transmission Line Resonator Model for Fast Extraction of Electromagnetic Properties of Cavities in Two-Dimensional Photonic Crystals

M. A. Miri
A. Khavasi, Member, IEEE
M. Miri
K. Mehrany, Member, IEEE
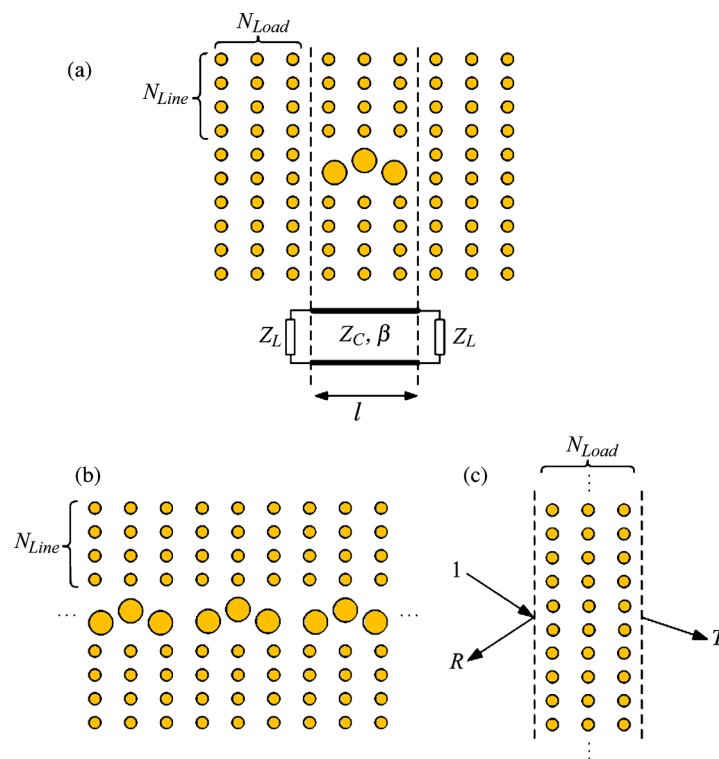
A Transmission Line Resonator Model for Fast Extraction of Electromagnetic Properties of Cavities in Two-Dimensional Photonic Crystals

M. A. Miri, A. Khavasi, *Member, IEEE*, M. Miri, and K. Mehrany, *Member, IEEE*

Sharif University of Technology, Tehran 11365-9363, Iran

Abstract: In this paper, photonic cavities made of point defects in 2-D photonic crystals are modeled by finite-size transmission lines terminated at both ends by appropriate scalar impedances. The proposed model forms a simple transmission line resonator and is demonstrated to be quite beneficial in fast extraction of resonant frequency, quality factor, and mode profile of such photonic cavities. In this manner, an approximate yet quite accurate approach is introduced to characterize the electromagnetic properties of photonic crystal cavities. This method is successfully applied to different structures for both major polarizations and is shown to be as accurate as rigorous numerical methods, viz. the finite-element method.

Index Terms: Photonic crystals.

1. Introduction

It is a well-known fact that introducing a point defect in a photonic crystal forms a microcavity with resonance frequencies lying within the band gap of the photonic crystal [1], [2]. Miscellaneous methods that have been thus far reported to analyze such defect modes can all be classified into either of the following categories: 1) rigorous numerical methods or 2) semi-analytical approaches. The former category includes well-known fully numerical methods, viz. the finite-difference time domain (FDTD) [2] or the finite-element method (FEM) [3]. These numerical methods are quite accurate but incur a heavy computational burden. The latter category includes those methods that are usually based on the expansion of electromagnetic fields in terms of different basis functions, e.g., plane waves in a supercell [4], [5], oscillating dipole moments [6], or Wannier functions [7]. Semi-analytical methods in the second category are, however, not always rigorous and sometimes comprise approximate yet accurate enough methods like the one proposed in [8], where geometrical optics is invoked to extract the resonance frequency of hollow cavities by using the fact that the round-trip phase of optical rays within the cavity should be an integer multiple of 2π. This approach is shown to be quite accurate but works only in those photonic crystal cavities that trap the electromagnetic energy in a homogeneous region surrounded by periodic variation of the refractive index, e.g., in point defects formed by removal of rods in conventional photonic crystals. Even in such cavities, it is incapable of rendering either the quality factor or the mode profile.

It is the intention of this work to present an approximate semi-analytical method to describe the most important electromagnetic properties of photonic crystal cavities, i.e., the resonance frequency together with the quality factor and mode profile, in an accurate and insightful manner. To this end, the concept of impedance matching in a transmission line is employed to extend the idea of in-phase adding up of optical rays in a round trip, and thus, the most general form of photonic cavities made of arbitrary point defects in 2-D photonic crystals is successfully analyzed. The concept of impedance matching has been already employed in design of photonic crystal circuits [9]–[11] and in calculation of reflection coefficients from the photonic crystal interfaces [12], [13] but has been never brought into play for modeling of point defects as photonic crystal resonators. Here, the defect region is first replaced by a transmission line whose electromagnetic characteristics correspond to those of the photonic crystal waveguide which is formed by making a line defect out of the original point defect, i.e., by periodic repetition of the defect region along either of the two axes of periodicity in the 2-D photonic crystal. This transmission line is then terminated at both ends with an impedance whose normalized value is obtained by calculating the electromagnetic reflection from the photonic crystal adjacent to the defect zone. In this fashion, a very simple transmission-line resonator is formed, and the resonance frequency of the structure is calculated by finding the frequency at which the ends of the line are matched. The quality factor of the structure is estimated by using the half-power bandwidth of the impedance seen from the input of the line. Finally, the mode profile is extracted by using the propagation constant of the transmission line and the field profile of its corresponding photonic crystal waveguide. It is, however, worth noticing that all our calculations are made by using scalar values and, thus, do not consider higher orders of diffraction within the photonic crystal. This, however, is not a serious detriment because the expected working frequencies are within the gap, and we have no pro-pagating Floquet orders in the periodic region.

The organization of the paper is as follows: The details of the proposed method are presented in Section 2, where the calculation of resonance frequency, quality factor, and mode profile are all explained. Different numerical examples are provided in Section 3, and conclusions are made in Section 4.

2. Proposed Transmission-Line Resonator Model

A typical photonic crystal cavity created by an arbitrary point defect in a finite-size photonic crystal is shown in Fig. 1(a). The defect region is modeled by a transmission line whose characteristic impedance, propagation constant, and length are denoted by Z_C, β, and l, respectively.

The propagation constant of the transmission line is made equal to that of the photonic crystal waveguide, which is shown in Fig. 1(b). This line-defect waveguide is created by the periodic repetition of the defect region along either of the two axes of periodicity in the original structure [see the abscissa in Fig. 1(b)]. It is worth noticing that there are only N_{Line} rows of rods at the upper and lower neighborhoods of the defect region, and thus, the photonic crystal waveguide is lossy and has a complex propagation constant:

$$\beta(\omega) = \beta_r(\omega) - j\beta_i(\omega) \tag{1}$$

The imaginary part of the propagation constant β_i has a contribution in decreasing the overall Q factor of the cavity and is negligible only if N_{Line} is large enough to insure total reflection. The calculation of the propagation constant of the waveguide is a straightforward problem and could be accomplished by a variety of rigorous methods [14]–[16]. It is worth noticing that extraction of the sought-after propagation constant is also possible by using approximate methods based on physical optics [17] or scalar impedance theory [18].

The characteristic impedance Z_C is determined together with the load impedance Z_L. It should be noticed that the value of the characteristic impedance itself is not needed as long as the normalized value of the load impedance $\overline{Z}_L = Z_L/Z_C$ is known. Fortunately, the sought-after normalized impedance can be easily determined by calculating the reflection coefficient from the photonic crystal shown in Fig. 1(c). This photonic crystal is composed of N_{Load} columns of rods and is
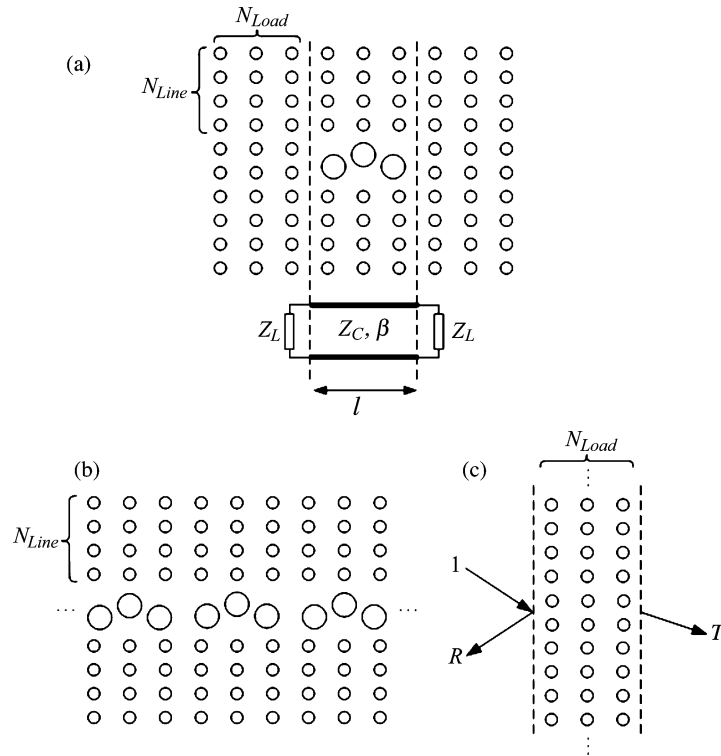
Fig. 1. Arbitrary point defect in a 2-D photonic crystal cavity and its corresponding transmission line resonator. (a) General structure and its overall model. (b) Line-defect waveguide for extraction of the transmission-line propagation constant. (c) Surrounding photonic crystal for extraction of the load impedance to terminate the line.

assumed fully periodic along the other axis perpendicular to the line defect [see the ordinate in Fig. 1(c)]. The normalized impedance is then written as

$$\frac{Z_L(\omega)}{Z_C} = \frac{1 + R(\omega)}{1 - R(\omega)} \tag{2}$$

where $R(\omega)$ stands for the reflection coefficient of an incident plane wave coming from free space and having its normal component of wave-vector tuned at the propagation constant of the line-defect mode β. The noninfinite nature of the photonic crystal thickness in Fig. 1(c) is one other factor in decreasing the overall Q factor of the resonator. However, if N_{Load} is large enough to insure total reflection, then the normalized impedance becomes pure imaginary, and there will be no resistive term to decrease the Q factor. Here, a Fourier-based method is followed to extract the sought-after reflection coefficient [19].

It should be noticed that even though estimation of the normalized impedance by using the reflection coefficient of uniform plane waves being incident from free space sounds dubious, tuning the normal component of its wave-vector is proved to be corrective, and the obtained results are almost always satisfactory. This could be explained by the fact that the zeroth-order space harmonic of the nonuniform incident wave coming from the line-defect region is the decisive factor in the determination of the overall reflection coefficient, particularly when the frequency of the wave lies within the band gap of the photonic crystal [20].

Having the propagation constant of the transmission line in the proposed model and the normalized impedance of the load, it is now straightforward to extract the resonance frequency and quality factor of the cavity.
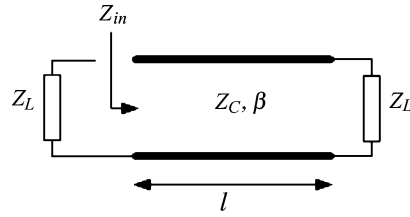
Fig. 2. Transmission-line resonator model for calculation of the resonance frequency and quality factor.

2.1. Extraction of Resonance Frequency and Quality Factor

The proposed transmission-line resonator model is schematically shown in Fig. 2. The normalized input impedance seen from the left terminal of the transmission line can be easily written as [21]

$$\overline{Z_{in}}(\omega) = \frac{\overline{Z_L}(\omega) + \tan(\beta(\omega)l)}{1 + \overline{Z_L}(\omega)\tan(\beta(\omega)l)} \tag{3}$$

where β and $\overline{Z}_L$ are already determined, and l is the length of the transmission line. It is by making the imaginary part of the normalized input impedance, i.e., $Im\{\overline{Z_{in}}(\omega_0)\}$, equal to the imaginary part of the complex conjugate of the normalized load impedance, i.e., $Im\{\overline{Z_{in}}^*(\omega_0)\}$, that the resonance frequency ω_0 can be extracted.

The dispersion equation governing the eligible resonance frequencies can then be written as

$$Im\{\overline{Z_{in}}(\omega_0)\} = -Im\{\overline{Z_L}(\omega_0)\}. \tag{4}$$

It is worth noticing that the aforementioned equation can have more than one root each corresponding to a specific cavity mode.

The quality factor corresponding to a specific resonance frequency ω_0 can then be easily found by calculation of the half-power bandwidth BW of the total impedance, i.e., $\overline{Z_{in}}(\omega) + \overline{Z_L}(\omega)$, in the transmission line resonator shown in Fig. 2. Once the absolute value of the total impedance is plotted and the half-power bandwidth is extracted, the quality factor can be written as

$$Q = \frac{f_0}{BW}. \tag{5}$$

As already mentioned, there are two different factors at work in lowering the quality factor: First, we have the imaginary part of propagation constant β_i. This factor accounts for the leakage due to the presence of only a limited number of rows N_{Line}. Second, we have the resistive nature of the load impedance, which is due to the presence of only a limited number of columns N_{Load}.

2.2. Calculation of Mode Profile

Regarding the fact that the defect region in the photonic crystal is modeled by a finite-size transmission line, the field profile within the cavity can be written as the superposition of forward and backward modes supported by the line-defect waveguide in Fig. 1(b). Therefore, the wave function within the defect region reads as

$$\psi = \psi_0 \left\{ \Phi(x, y)e^{-j\beta x} + R\Phi(-x, y)e^{j\beta x} \right\} \tag{6}$$

where ψ_0 is an arbitrary constant, R is the reflection coefficient in (2), $\Phi(x, y)$ is the periodic function corresponding to the mode profile of the defect-line waveguide, β is the propagation constant, and finally, ψ is either E_z or H_z for E and H polarized waves, respectively. Whenever there is an even
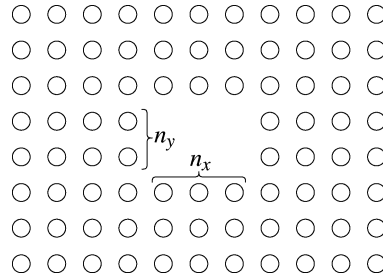
Fig. 3. Structure of the first example.

TABLE 1

Resonant frequencies of different point-defect cavities in the first example.

$n_x \times n_y$	1×1	1×2	1×3	2×1	2×2	2×3	3×1	3×2	3×3
Proposed method	$f_{00} = 0.3945$	$f_{00} = 0.3546$ $f_{01} = 0.4302$	$f_{00} = 0.3390$ $f_{10} = 0.3874$ $f_{20} = 0.4451$	$f_{00} = 0.3546$ $f_{10} = 0.4302$	$f_{01} = 0.3967$ $f_{10} = 0.3969$	$f_{10} = 0.3397$ $f_{01} = 0.3829$ $f_{20} = 0.4207$ $f_{11} = 0.4287$	$f_{00} = 0.3390$ $f_{01} = 0.3874$ $f_{02} = 0.4451$	$f_{01} = 0.3397$ $f_{10} = 0.3829$ $f_{02} = 0.4207$ $f_{11} = 0.4287$	$f_{01} = 0.3200$ $f_{10} = 0.3202$ $f_{11} = 0.3784$ $f_{02} = 0.4088$ $f_{20} = 0.4090$ $f_{12} = 0.4490$ $f_{21} = 0.4490$
FEM	$f_{00} = 0.3945$	$f_{00} = 0.3544$ $f_{01} = 0.4299$	$f_{00} = 0.3389$ $f_{10} = 0.3874$ $f_{20} = 0.4448$	$f_{00} = 0.3544$ $f_{10} = 0.4299$	$f_{01} = 0.3966$ $f_{10} = 0.3966$	$f_{10} = 0.3394$ $f_{01} = 0.3826$ $f_{20} = 0.4204$ $f_{11} = 0.4284$	$f_{00} = 0.3389$ $f_{01} = 0.3874$ $f_{02} = 0.4448$	$f_{01} = 0.3394$ $f_{10} = 0.3826$ $f_{02} = 0.4204$ $f_{11} = 0.4284$	$f_{01} = 0.3200$ $f_{10} = 0.3200$ $f_{11} = 0.3781$ $f_{02} = 0.4087$ $f_{20} = 0.4087$ $f_{12} = 0.4486$ $f_{21} = 0.4486$

symmetry in the permittivity of the structure, however, the field profile will be symmetric too [22], and the mode profile can be written as

$$\psi = \psi_0 \Phi(x, y) e^{-j\beta x} \{1 \pm R e^{j2\beta x}\}. \tag{7}$$

This expression yields the mode profile in terms of the field profile in the line-defect waveguide of Fig. 1(b), its propagation constant, and the reflection coefficient in (2). For the number of nodes in the abscissa and ordinate directions, it is quite instructional to have the cavity mode number, and it is found by inspection of the mode profile in (6). It is worth noticing that even though the total number of vertical nodes are determined only by looking at $\Phi(x, y)$, the total number of horizontal nodes depend on both $\Phi(x, y)$ and R.

3. Examples and Discussion

Various numerical examples are discussed in this section. First, a square lattice of dielectric rods in air is considered. Dielectric rods have the relative permittivity of 8.9 and radius of 0.2 times the lattice constant. In accordance with Fig. 3, the point-defect cavity is formed by removing an array of $n_x \times n_y$ rods in a photonic crystal with $N_{Line} = 3$ and $N_{Load} = 4$.

The E-polarized resonance frequency of the ijth mode supported by this structure is denoted by f_{ij} and is tabulated in Table 1, where the resonance frequencies are normalized to the ratio of light velocity to lattice constant and are given for different values of n_x and n_y. They are obtained by following the rigorous FEM and the proposed method. An excellent agreement is observed between the two, and the encountered error is always smaller than 0.2% of the band gap width.

It should be noticed that the f_{ij} for the cavity carved by removing an array of $n_x \times n_y$ rods and the f_{ji} for the cavity carved by removing an array of $n_y \times n_x$ rods are expected to be equal. Nevertheless, the obtained result for the latter case is not necessarily equal to the obtained result for the former case because the line defect used for the transmission line is, in one case, constructed along the
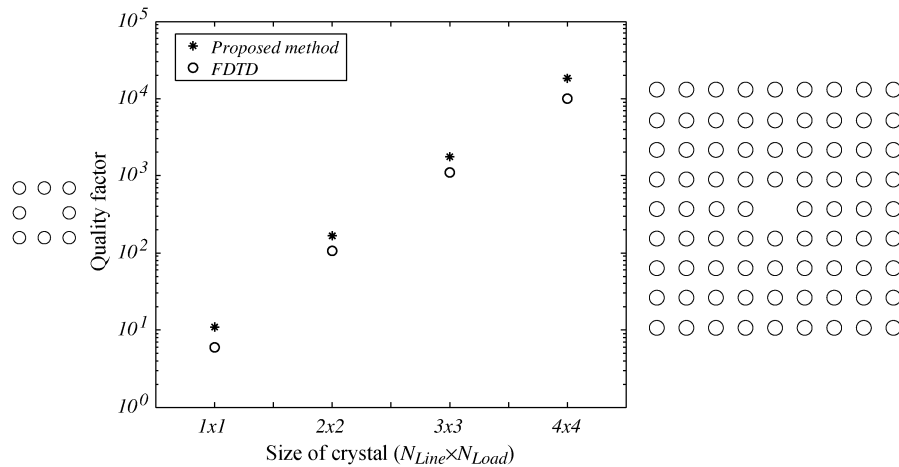
Fig. 4. Quality factor of point-defect cavities versus $N_{Line} \times N_{Load}$.

ordinate and the other along the abscissa. This table, however, proves that in the presented example, it does not matter which axis is to be employed for construction of the transmission line.

It should be also noticed that sometimes, the existence of higher order modes are not solely due to the existence of more than one root for (4); rather, the line-defect waveguide could have several modes, each yielding a transmission line supporting one or several resonance frequencies.

As the second example, the quality factor for the 1×1 cavity carved in the same photonic crystal is calculated for different values of N_{Line} and N_{Load}. The results obtained by using the proposed method and the FDTD are plotted in Fig. 4 versus $N_{Line} \times N_{Load}$.

This figure demonstrates that our calculated value for the quality factor is always an overestimation. This fact can be attributed to our assuming perfect periodicity for the photonic crystal in Fig. 1(c), when the normalized load impedance was to be calculated. This assumption neglects the vertical leakage of energy in the photonic crystal region outside of the cavity and, consequently, underestimates the loss.

As the third example, the original square lattice photonic crystal with $N_{Line} = 3$ and $N_{Load} = 4$ is considered, but the cavity is formed by replacing the array of $n_x \times n_y$ original dielectric rods with new ones having normalized radius of 0.34. Interestingly, the corresponding waveguide supports two modes: one with even symmetry and a negative group velocity and the other with odd symmetry with a positive group velocity.

Once again, the E-polarized resonance frequency of the ijth mode is calculated for different values of $n_x \times n_y$. The results are summarized in Table 2, where one of the columns is devoted to the results obtained by using the even-symmetric mode of the line defect and the other devoted to the results obtained by using the odd-symmetric mode of the line defect.

Perusal of the data in this table indicates that the proposed method in this example has become more erroneous when the accuracy of its results is compared against that of the previous example. Nevertheless, the accuracy in determination of resonance frequencies never exceeds the 3% of photonic band gap width. The reduction of accuracy in this example can be explained by pointing out that the introduction of larger rods as point defects has enhanced the spatial harmonic contents of the field profile and, thus, has deteriorated the accuracy of relying only on the fundamental Bloch order for extraction of electromagnetic properties.

Furthermore, the degeneracy of the resonance frequencies $f_{01} = f_{10} = 0.3705$ in the 1×1 cavity is destroyed. These two degenerate modes are estimated with $f_{01} = 0.3749$ and $f_{10} = 0.3680$.

All three cavities in this example are modeled with the same transmission line and the same termination load. It is the length of the transmission line that is different in every one of those cavities. The rigorous steps, viz. determination of transmission line characteristics and the scalar impedances, are not necessarily to be repeated in different configurations.

TABLE 2

Resonant frequencies of different point-defect cavities in the third example.

$n_x \times n_y$	Odd mode of the line-defect		Even mode of the line-defect	
	Proposed method	FEM	Proposed method	FEM
1×1	$f_{01} = 0.3749$	$f_{01} = 0.3705$	$f_{10} = 0.3680$	$f_{10} = 0.3705$
2×1	$f_{01} = 0.3653$ $f_{11} = 0.3847$	$f_{01} = 0.3623$ $f_{11} = 0.3809$	$f_{10} = 0.3487$ $f_{30} = 0.4020$	$f_{10} = 0.3506$ $f_{30} = 0.3983$
3×1	$f_{01} = 0.3606$ $f_{11} = 0.3746$ $f_{21} = 0.3876$	$f_{01} = 0.3590$ $f_{11} = 0.3713$ $f_{21} = 0.3856$	$f_{10} = 0.3375$ $f_{30} = 0.3753$ $f_{50} = 0.4142$	$f_{10} = 0.3411$ $f_{30} = 0.3754$ $f_{50} = 0.4110$
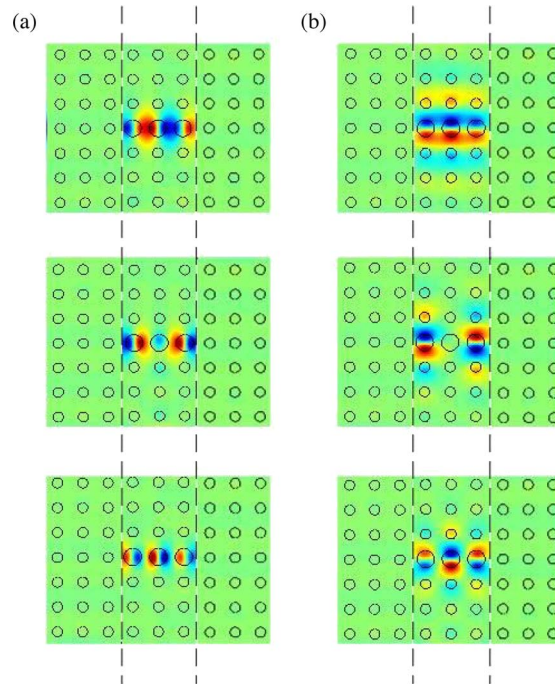
Fig. 5. Mode profile of six different modes from the proposed method. (a) TE$_{10}$, TE$_{30}$, and TE$_{50}$ from top to bottom. (b) TE$_{01}$, TE$_{11}$, and TE$_{21}$ from top to bottom.

To demonstrate the feasibility of (7) in obtaining the mode profile within the defect region, six different modes supported by the 3×1 cavity in this example, i.e., TE$_{01}$, TE$_{11}$, TE$_{21}$, TE$_{10}$, TE$_{30}$ and TE$_{50}$, are considered, and their mode profiles are plotted in Fig. 5. The defect region is specified by dashed lines in this figure. The even and odd symmetry of these mode profiles are quite obvious. These mode profiles are, by the way, validated by using the FEM in Fig. 6. The similarity between the proposed approach and the FEM is quite obvious.

As the final example, a triangular lattice composed of dielectric rods in air is considered. The relative permittivity of rods is 11.4, and their radius is 0.35 times the lattice constant. By following
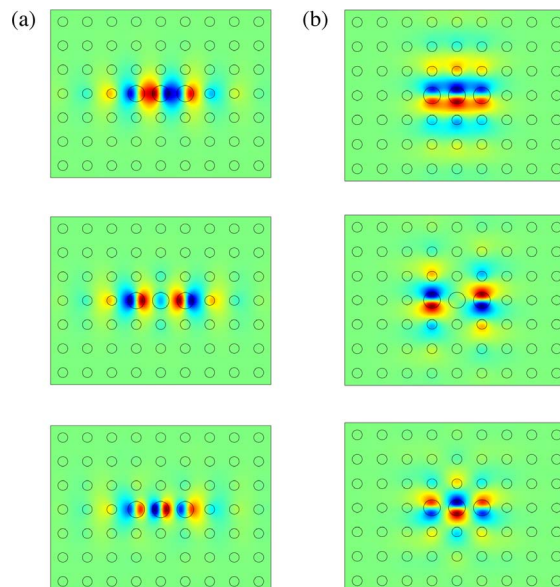
Fig. 6. Mode profile of six different modes from the FEM. (a) TE_{10}, TE_{30}, and TE_{50} from top to bottom. (b) TE_{01}, TE_{11}, and TE_{21} from top to bottom.

TABLE 3

Resonant frequencies of different point-defect cavities in the final example.

$n_x \times n_y$	Proposed Method	FEM
1×1	$f_{00} = 0.3244$	$f_{00} = 0.3228$
2×1	$f_{00} = 0.3181$ $f_{10} = 0.3394$	$f_{00} = 0.3169$ $f_{10} = 0.3383$
3×1	$f_{00} = 0.3142$ $f_{10} = 0.3292$ $f_{20} = 0.3486$	$f_{00} = 0.3136$ $f_{10} = 0.3272$ $f_{20} = 0.3474$

the same line, the resonance frequencies, this time for H polarized modes, are tabulated in Table 3. Once again, a very good agreement is observed.

4. Conclusion

A simple transmission-line resonator model for extraction of resonant frequency, quality factor, and mode profile of 2-D photonic crystal cavities has been introduced. It was shown to be applicable for both major polarizations. The presented results were justified by using either the FDTD or the FEM. It was shown that the quality factor obtained by following the proposed method is always an overestimation of the actual value. The presented method was also shown to be very accurate in those cases where the defect region is formed by removal of rods in photonic crystals.

It should be noticed that even though the horizontal axis was chosen to build the line-defect waveguide for forming the transmission line of the proposed model in Section 2, one can exchange

the horizontal and vertical coordinates in Fig. 1 and obtain a similar model with different parameters. Interestingly, it was shown that both these models give virtually corresponding results. Further investigation of these points shows that the discrepancy between the results of those models is not conspicuous but is for those cases where N_{Load} and N_{Line} are quite small.

References

[1] J. D. Joannopoulos, S. G. Johnson, J. N. Winn, and R. D. Meade, *Photonic Crystals Molding the Flow of Light,* 2nd ed. Princeton, NJ: Princeton Univ. Press, 2008.

[2] P. R. Villeneuve, S. Fan, and J. D. Joannopoulos, "Microcavities in photonic crystals: Mode symmetry, tunability and coupling efficiency," *Phys. Rev. B, Condens. Matter*, vol. 54, no. 11, pp. 7837–7842, Sep. 1996.

[3] V. F. Rodriguez-Esquerre, M. Koshiba, and H. E. Hernandez-Figueroa, "Finite-element analysis of photonic crystal cavities: Time and frequency domains," *J. Lightw. Technol.*, vol. 23, no. 3, pp. 1514–1521, Mar. 2005.

[4] K. Sakoda, *Optical Properties of Photonic Crystals*. New York: Springer-Verlag, 2001.

[5] E. Yablonovitch, T. J. Gmitter, R. D. Meade, A. M. Rappe, K. D. Brommer, and J. D. Joannopoulos, "Donor and acceptor modes in photonic band structure," *Phys. Rev. Lett.*, vol. 67, no. 24, pp. 3380–3383, Dec. 1991.

[6] K. Sakoda and H. Shiroma, "Numerical method for localized defect modes in photonic lattices," *Phys. Rev. B, Condens. Matter*, vol. 56, no. 8, pp. 4830–4835, Aug. 1997.

[7] A. Martin, D. Hermann, F. Hagmann, K. Busch, and P. Wolfle, "Defect computations in photonic crystals: A solid state theoretical approach," *Nanotechnol.*, vol. 14, no. 2, pp. 177–183, 2003.

[8] E. Istrate, A. A. Green, and E. H. Sargent, "Behavior of light at photonic crystal interfaces," *Phys. Rev. B, Condens. Matter*, vol. 71, no. 19, p. 195122, 2005.

[9] S. Boscolo, C. Conti, M. Midrio, and C. G. Someda, "Numerical analysis of propagation and impedance matching in 2-D photonic crystal waveguides with finite length," *J. Lightw. Technol.*, vol. 20, no. 2, pp. 304–310, Feb. 2002.

[10] S. Boscolo, M. Midrio, and T. F. Krauss, "Y junctions in photonic crystal channel waveguides: High transmission and impedance matching," *Opt. Lett.*, vol. 27, no. 12, pp. 1001–1003, 2002.

[11] S. Boscolo, M. Midrio, and C. G. Someda, "Coupling and decoupling of electromagnetic waves in parallel 2-D photonic crystal waveguides," *IEEE J. Quantum Electron.*, vol. 38, no. 1, pp. 47–53, Jan. 2002.

[12] R. Biswas, Z. Y. Li, and K. M. Ho, "Impedance of photonic crystals and photonic crystal waveguides," *Appl. Phys. Lett.*, vol. 84, no. 8, pp. 1254–1256, 2004.

[13] B. Momeni, A. A. Eftekhar, and A. Adibi, "Effective impedance model for analysis of reflection at the interfaces of photonic crystals," *Opt. Lett.*, vol. 32, no. 7, pp. 778–780, 2007.

[14] Q. Chen, Y. Z. Huang, W. H. Guo, and L. J. Yu, "Calculation of propagation loss in photonic crystal waveguides by FDTD technique and Padé approximation," *Opt. Commun.*, vol. 248, no. 4–6, pp. 309–315, Apr. 2005.

[15] K. Yasumoto, *Electromagnetic Theory and Application of Photonic Crystals*. Boca Raton, FL: CRC, 2006.

[16] A. Theocharidis, T. Kamalakis, and T. Sphicopoulos, "Analysis of photonic crystal waveguide discontinuities using the mode matching method and application to device performance evaluation," *J. Opt. Soc. Amer. B, Opt. Phys.*, vol. 24, no. 8, pp. 1698–1706, 2007.

[17] E. Istrate and E. H. Sargent, "Photonic crystal waveguide analysis using interface boundary conditions," *IEEE J. Quantum Electron.*, vol. 41, no. 3, pp. 461–467, Mar. 2005.

[18] A. Khavasi, N. Habibi, A. H. Hosseinnia, and K. Mehrany, "A transmission line model for extraction of defect modes in two-dimensional photonic crystals," in *Proc. ICP*, 2010, accepted for publication.

[19] A. Khavasi, A. K. Jahromi, and K. Mehrany, "Longitudinal Legendre polynomial expansion of electromagnetic fields for analysis of arbitrary-shaped gratings," *J. Opt. Soc. Amer. A, Opt. Image Sci.*, vol. 25, no. 7, pp. 1564–1573, Jul. 2008.

[20] M. Miri, A. Khavasi, K. Mehrany, and B. Rashidian, "Transmission-line model to design matching stage for light coupling into two-dimensional photonic crystals," *Opt. Lett.*, vol. 35, no. 2, pp. 115–117, 2010.

[21] R. E. Collin, *Foundations for Microwave Engineering*, 2nd ed. Piscataway, NJ: IEEE Press, 2001.

[22] T. Tamir, *Integrated Optics,* 2nd ed. New York: Springer-Verlag, 1985.